

Manuscript Number: CENG-D-16-00016R1

Title: A Parametric Model For Barred Equilibrium Beach Profiles: Two-dimensional Implementation

Article Type: Research Paper

Keywords: bathymetry estimation
remote sensing
nearshore
equilibrium beach
parametric profiles

Corresponding Author: Prof. Robert A. Holman,

Corresponding Author's Institution: College of Oceanography

First Author: Robert A. Holman

Order of Authors: Robert A. Holman; David Lalajini; Todd Holland

Abstract: A method is proposed for estimating approximate 2DH bathymetry including longshore variable shoreline and sand bar systems. The method is based on, but extends, a previous 1DH model of Holman et al [2014] by assuming that this 1DH equilibrium barred bathymetry can be applied for any offshore location if the corresponding mean shoreline orientation is taken to be the local average over a longshore span that is K times the offshore distance. Thus locations close to the beach are sensitive to shoreline and bar details while more seaward locations are steadily less sensitive.

The model was tested against 14 ground truth surveys, collected over two years and under widely ranging environmental condition, spanning a 500 by 1000 m region. Models inputs for the shoreline and sand bar positions were extracted from measured bathymetries for these tests (but would be derived from other sources in real applications) while deep-water inputs were found from a single deep-water survey. The model yielded complete 2DH bathymetry maps that were a very good approximation of ground truth. The mean bias and rms error over the full region and data set were 0.27 m and 0.49 m respectively and proxy bathymetries were visually very similar to ground truth. The largest source of error was occasional cross-shore misplacements of otherwise realistic looking sand bars. Results were only weakly dependent on the value of K when tested over a factor of four and the default value of 1.0 is recommended. Performance statistics using input locations for the shoreline and bar crest that were manually digitized from breaking patterns in rectified optical time exposure images were no worse than bathymetry-based inputs. Hydrodynamic predictions using these bathymetries would be a substantial improvement over those from monotonic or even barred 1DH equilibrium proxy bathymetries.

We would like to thank the reviewers for interesting and helpful comment. We feel the paper has certainly been improved. Specific comments and responses follow.

Reviewers' comments:

Reviewer #1.

1. The authors proposed that a transect is set to be perpendicular to the shoreline orientation locally averaged alongshore. However, the results are insensitive to the K value, which determines the alongshore distance of the averaging. These results seem to show that to set a transect perpendicular to the shoreline orientation averaged in the whole domain or in the fixed distance, which does not vary according to the distance between a target point to the shoreline, would also work well and this method is simpler than that the authors proposed.

This is an interesting issue that made me realize that the HLEV14 results are just what the reviewer suggests, 1DH comparisons of offshore oriented profiles with no attention paid to the shoreline orientation. So apparently this is not a terrible option for a relatively straight beach. However, there are two issues that favor the 2D implementation. First, every fluctuation in the shoreline location yields an equal fluctuation in offshore features, so for example the crest of an offshore sand bar several hundred meters from the shoreline would oscillate in the cross-shore direction just as much as the shoreline does. This seems aphysical (offshore features do not fluctuate in the cross-shore to the same extent or at the short longshore scales that the shoreline does), but doesn't introduce big errors since offshore features are usually low-sloping. More important would be cases where the shoreline has more curvature so that cross-shore direction clearly varies along the beach (for instance for an embayed beach). In this case, ignoring this variation would yield large errors. We have included text after figure 9 (new figure count) summarizing this point.

2. The authors pointed out that the estimation error in elevation mainly resulted from the error in the input bar crest position. It seems to me that the foreshore slope ϕ_s and the water depth of the seaward limit of the active bar zone h_{sea} , which were determined in HLEV14 using the survey data and a kind of trial and error method, respectively, are difficult to estimate and may include relatively large errors in particular where survey data is limited.

Hence, in order to understand how sensitive the five input parameters are to the results, sensitivity tests for the five parameters are recommended. Although a sensitivity test for h_{sea} was conducted in HLEV14, the comparison of the five test results might be useful.

Fair point. We have expanded the discussion to include content on the sensitivity to all of the inputs including the addition of two new figures showing the sensitivities to the shoreline and offshore bathymetric slopes. Surprisingly, overly flat offshore slopes have the largest impact because they cause the shallow water region where bars are present to

be limited to a very narrow spatial region (therefore with only minor bar perturbations).

3. Figures showing comparisons between measured and estimated profiles on October 21, 2009, September 16, 2009 and April 15, 2010 might be helpful for readers to recognize the differences between the measurements and estimations.

Both reviewers suggested this and I have included a new figure 5 with cross-shore transects from October 21, 2009, to support the map comparisons in Figure 3. Note that the transects were investigated more thoroughly in HLEV14 since that paper dealt exclusively with 1DH predictions.

Reviewer #2: Review of paper by Holman, R.A., Lalejini, D.M., and Holland, T.: "A parametric model for barred equilibrium beach profiles: Two-dimensional implementation"

The authors are requested to address the following comments of a more general nature:

1. Explain the method developed further. It is a bit hard to understand the way the longshore variation in the model is derived, both in the abstract and the text - please expand a bit. Is a depth at a certain point the result of an averaging for several EBP or only one? Is there a problem with overlapping transects? How is the bar feature affected by the method?

This is a bit tricky but is the heart of the paper so worth clarity. I have re-written and expanded section 2.2 somewhat to clarify and I refer specifically and carefully to Figure 1 to illustrate how this works in a step-by-step way. Just to clarify for the reviewer, this is NOT the average of profiles that radiate from the shoreline at orientations that depend on the local shoreline orientation. That is what we first tried and it failed (this is also noted in the text in this section). Instead, we look shoreward from each individual offshore point (specified in an output grid) to find an average shoreline orientation seen from that point, then find the 1D equilibrium profile along that transect using HLEV14. This makes the result unique for every point and also smoothly varying in space. I considered modifying the abstract to clarify this procedure, but I don't think there is a sufficiently compact version that would be abstract-appropriate.

2. Specify limitations to the EBP equations. The equations used to calculate the EBP contain a large number of empirical parameters. More discussion on the range of validity of these parameters and the balance between them (robustness of predictions; possible correlations between parameters etc) would be useful. I realize that such information might be available in previous papers, but I feel this should be discussed in this paper as well.

I have included a deeper discussion of the sensitivity to these parameters in the discussion based on both reviewers comments. Two new figures have been added to illustrate the

sensitivity to the shoreline and offshore slopes.

3. Comment on the case of multi-bar profiles. I suppose the EBP profile is only applicable to single bar profiles. Typically two bars are present at Duck, so some comments with regard to this limitation and the application to the present data set is warranted.

In fact, the algorithm automatically predicts multiple bars including the typical two bars at Duck. This comes from the cosine term in the equation that is applied between the shoreline and seaward depth, h_{Sea} . This is a nice result of the Ruessink paper (you don't have to worry about how many bars are present).

4. Show comparisons for individual profiles. The figures displayed in the paper all focus on the complete bathymetry. This is fine; however, it would be interesting to shown a couple of comparisons for profiles as well to indicate how realistically the derived profile shape is, especially in the bar region.

This was also suggested by the other reviewer. While this was the focus of the HLEV14 paper, I have added some example profiles in the new Figure 5 to better illustrate the model performance (see also reviewer 1 point 3).

5. Discuss practical aspects of applying the model. Although the applicability of the model and the procedure to employ it is discussed in some places in the paper, I would like to see a more thorough and coherent discussion of this. Also, it would be worthwhile to try to point out useful engineering applications of the model.

Good suggestion. I have added material on practical applications in the discussion section.

Specific comments

In the following specific comments are given to the paper.

Introduction Would be nice to refer to Bruun when you discuss the EBP. Also to add Inman, Elwany, and Jenkins (they derived a composite EBP).

Both references added in the first para of the intro.

Equation 1 A t should be an x , right?

Yes. Good catch.

Section 2.1 Any physically based motivation for a planar slope in the offshore?

The hypothesis from HLEV14 was that wave-driven processes cause a concave up profile in the nearshore but that larger scale geological processes take over across the rest of the

shelf. Most EBPs are concave up at all x , so eventually flatten out (unrealistically) at large x . We felt this was unreasonable and that a planar offshore was more realistic. That said, most applications of this EBP will be nearshore, so the offshore details are not very important.

Equation 2 What is the interpretation of alpha in the equation? Define and specify where x originates.

This is from HLEV14 and represents a general form for a linear and exponential superposition. Alpha is needed so that the shoreline can be anywhere, i.e. h can go to zero at any specified x – once the shoreline is specified, alpha is found from this equation. So it doesn't have a physical interpretation other than the offset needed to allow the shoreline to be defined.

Equation 3 Not easy to grasp the essence of this equation. Any possibility to add some explanation to the chosen form?

Fair question. It is from the Ruessink paper and is really just a fancy form of a cosine wave, but with a spatially variable wavelength and amplitude). I rewrote the explanatory paragraph immediately after equation (3) to make this clearer. This is also described around equations 6 through 8.

Discussion The shoreline and bar crest locations are needed as input. The former is easy to obtain, but the latter not trivial. If you do not have survey data or images of breaking wave pattern, how would you employ your model, especially with regard to the bar crest location (see general comment 5 above)?

I have added some material in the discussion about practical applications of this model and have included sentences on this topic. In short, the algorithm will make realistic sand bars no matter what, but their cross-shore position will depend on whatever phase ($\psi(t)$) you input. So you will get realistic looking bars and even resulting hydrodynamics, and you can actually input any bar position you would like, perhaps exploring sensitivities to this input. There is no wrong answer since there is no ground truth to compare against.

- This paper describes a simple parametric methods for estimating realistic bathymetries that includes alongshore-variable shorelines and sand bars.
- The model is based on a parametric description of the sand bar envelope published by Ruessink et al [2003] and is an extension of a 2014 Coastal Engineering 1DH version by Holman et al [2014].
- The model requires only specification of the location and climatological slope of the shoreline, the location of a sand bar, and the depth and slope of some deep water contour seaward of the region of active sand bar activity.
- Tests against 14 ground truth surveys at Duck, NC, yield bathymetries that match well the survey data with a global bias of 0.27 and rms error 0.49 m. Roughly 90% of estimates lie within 0.86 m of ground truth.

A Parametric Model For Barred Equilibrium Beach Profiles:
Two-dimensional Implementation

Robert A. Holman¹, David M. Lalejini² and Todd Holland³
Both at Marine Geosciences Division
Naval Research Laboratory
Code 7434, Bldg 1005
Stennis Space Center MS 39529-5004
USA

¹holman@coas.oregonstate.edu, ²David.Lalejini@nrlssc.navy.mil,
³Todd.Holland@nrlssc.navy.mil

Abstract

A method is proposed for estimating approximate 2DH bathymetry including longshore variable shoreline and sand bar systems. The method is based on, but extends, a previous 1DH model of Holman et al [2014] by assuming that this 1DH equilibrium barred bathymetry can be applied for any offshore location if the corresponding mean shoreline orientation is taken to be the local average over a longshore span that is K times the offshore distance. Thus locations close to the beach are sensitive to shoreline and bar details while more seaward locations are steadily less sensitive.

The model was tested against 14 ground truth surveys, collected over two years and under widely ranging environmental condition, spanning a 500 by 1000 m region.

Models inputs for the shoreline and sand bar positions were extracted from measured bathymetries for these tests (but would be derived from other sources in real applications) while deep-water inputs were found from a single deep-water survey. The model yielded complete 2DH bathymetry maps that were a very good approximation of ground truth.

The mean bias and rms error over the full region and data set were 0.27 m and 0.49 m respectively and proxy bathymetries were visually very similar to ground truth. The largest source of error was occasional cross-shore misplacements of otherwise realistic looking sand bars. Results were only weakly dependent on the value of K when tested over a factor of four and the default value of 1.0 is recommended. Performance statistics using input locations for the shoreline and bar crest that were manually digitized from breaking patterns in rectified optical time exposure images were no worse than bathymetry-based inputs. Hydrodynamic predictions using these bathymetries would be

a substantial improvement over those from monotonic or even barred 1DH equilibrium proxy bathymetries.

Keywords: bathymetry estimation, remote sensing, nearshore, equilibrium beach, parametric profiles

1 Introduction:

Parametric forms for equilibrium beaches have been studied and used for many years as plausible proxies for bathymetry for cases where the true bathymetry is unknown or is only poorly known, or for long-term applications such as beach response to sea level rise where it is assumed that only the gross characteristics of a beach such as increasing depth and upward concavity are important (see Özkan-Haller and Brundidge [2007] for a recent review). One of the most common models is the ubiquitous $h = Ax^{2/3}$ form, first introduced by Bruun [1954] then popularized by Dean [e.g. 1991], where x and h are distance from shore and depth and A is a dimensional calibration constant. However, other forms soon followed. Inman et al [1993] suggested a version that joined two Dean-like profiles at the breakpoint, Larson and Kraus [1989] suggested a form that superimposed a planar shallow water component with an offshore Dean form, Özkan-Haller and Brundidge [2007] introduced a modification to further limit the influence of the planar component to shallow water, and Bodge [1992] and Komar and McDougal [1994] suggested exponential rather than power law forms as a preferred solution that exhibited finite slope at the shoreline and a desired concave up profile. All of these forms flattened to a horizontal surface offshore, hopefully well seaward of a zone in which they would be applied.

While all of these forms capture some characteristics of beaches, none can represent the near-ubiquitous presence of sand bars in the nearshore. Since wave dissipation is focused over bars, hydrodynamic predictions such as nearshore circulation or peak wave height made using beach profiles that omit these features will have limited value.

Ruessink et al [2003; hereafter RWHKvE03] investigated the possibility of deriving a parametric form for sand bar perturbations to a simple background profile by analyzing extensive data sets from six beaches around the world and developing a general equation (described in the section below) that represented sand bars in terms of a sinusoidal function with spatially varying amplitude and wavelength. This bar function, h_{bar} , is superimposed on an underlying background bathymetry, h_0 , that might be derived from long-term average data or from one of the equilibrium equations noted above. Thus the total bathymetry would be

$$h(x,t) = h_0(x) + h_{bar}(h_0,t) \quad (1)$$

where they assumed no longshore variability.

In 2014, Holman et al [2014; hereafter HLEV14] published a paper that merged the RWHKvE03 with a new background equilibrium form that combined an exponential, concave-up, nearshore form with a planar form offshore that better represents the steady deepening of the continental shelf seaward of the wave-influenced zone (method summarized in section 2 of this paper). This equation improved the bathymetric representation for the many beach profiles tested from Duck, NC, beaches in the Pacific Northwest of the US, and from a Gulf of Mexico beach. Moreover, predictions of nearshore wave heights and longshore currents were considerably improved over predictions made on equilibrium profiles without sand bars.

1
2
3
4 The principal limitation of HLEV14 is the restriction to longshore uniform cases. While
5
6 the paper suggests that “a 2DH morphology can reasonably be represented by an
7
8 integrated set of adjacent 1DH slices”, the details of this process turned out to not be
9
10 trivial.
11
12
13
14

15
16 The purpose of this paper is to extend HLEV14 to allow for alongshore-variable
17
18 bathymetry while maintaining simplicity of implementation and good fidelity with actual
19
20 measured bathymetries. The next section will summarize the HLEV14 method for 1D
21
22 barred beach representation. Section 3 will then introduce a method to extend the 1D
23
24 case for 2D beaches based only on longshore estimates of the same simple parameters as
25
26 were used in the 1D case. This is followed by a section testing the predictions against
27
28 measurements for 14 example surveys from the Field Research Facility (FRF) at Duck,
29
30 NC. Thereafter follow discussion and conclusions.
31
32
33
34
35
36

37 **2. Model Formulation**

38
39 Since the 2D model is just an implementation of HLEV14, the next section will describe
40
41 the 1D implementation from that paper while the following section will detail the new
42
43 steps needed to expand to 2D. The reader is referred back to HLEV14 for greater detail
44
45 on the 1D implementation.
46
47
48

49 **2.1 The 1D HLEV14 Profile Model**

50
51 The one-dimensional model requires specification of a background (unbarred) profile, h_0 ,
52
53 and a barred perturbation function, h_{bar} , (eq. 1). For the background profile, HLEV14
54
55 proposed a mix of an exponential shoreward component to represent the concave up
56
57
58
59
60
61
62
63
64
65

1
2
3
4 shapes of wave-formed profiles with a planar offshore region to represent geological
5
6 shelf processes seaward of the wave-influenced zone,
7

$$h_0 = \alpha + \beta x + \gamma \exp(-kx) . \quad (2)$$

11 where α , β , γ and k are empirical coefficients (β is dimensionless, α and γ have units m
12
13 and k has units m^{-1}). They referred to this as a composite profile.
14
15

16 The four unknown coefficients were estimated using the following four pieces of
17
18 information: 1, the shoreline position (essentially shifting to a shore-based coordinate
19
20 system); 2, an equilibrium beach slope at the shoreline; 3, The depth at a specified
21
22 position that is seaward of the active bar zone; and 4, the shelf slope at that location.
23
24

25 The values of α and β are found directly while the values for γ and k must be found
26
27 iteratively using equations (5) and (7) from HLEV14.
28
29
30
31
32
33

34 The parametric form for the depth-dependent sand bar perturbation is taken from
35
36 RWHKvE03
37

$$h_{bar}(h_0, t) = -S(h_0)R(t)\cos[\theta(h_0) - \psi(t)] . \quad (3)$$

41 The sand bar form is represented by the cosine and can be compared to the more
42
43 familiar form of a progressive ocean wave, $\cos[kx - \sigma t]$, where k and σ represent the
44
45 wavenumber and frequency of the wave. In this case, the spatial variability, kx , is
46
47 replaced by a spatial phase function, $\theta(h_0)$ (solved in equations 6 and 7 below), so is
48
49 not a function of x directly but instead is a function of mean depth, h_0 . The
50
51 movement of the bar in time, represented by σt in a progressive wave, is
52
53 represented by $\psi(t)$, a temporal phase function that is found by locating the bar
54
55
56
57
58
59
60
61
62
63
64
65

crest at any time of interest (or any other feature – see HLEV14). $S(h_0)$ and $R(t)$ multiply the cosine so represent the amplitude of the cosine wave and how it varies in space (S) and in time (R).

From extensive survey data from six beaches in three countries, RWHKvE03 developed analytical forms for S, R and θ . They found that bar amplitude changes over time were small (i.e. bars change position much more than they grow or decay), so $R(t)$ was set to 1.0. The spatial envelope of bar amplitude, $S(h_0)$ was well modeled by a skewed Gaussian of the form

$$S = \delta \frac{x}{x_{off}} + \left(S_{max} - \delta \frac{x_{max}}{x_{off}} \right) \exp \left[\frac{- \left\{ \left(1 - \frac{h_0 - h_{shore}}{h_{sea} - h_{shore}} \right)^a - b \right\}^2}{c} \right] \quad (4)$$

where their original equations have been modified to remove the need to compensate for survey error in modeling parametric bathymetries (see HLEV14).

Bar amplitude depends on depth, h_0 , everywhere in the transect rather than on x directly. The maximum amplitude of the Gaussian envelope is determined by S_{max} (RWHKvE03 adjusted S_{max} by a noise floor threshold, δ , taken empirically as 0.3 for survey data. Since there is no noise in parametric predictions, this is compensated for by the first term in eq 4). h_{shore} and h_{sea} are the landward and seaward limits of significant bar activity (amplitude $> \delta$) and h_{shore} can safely be set to zero for

parametric applications. a , b and c are found empirically to be 0.53, 0.57 and 0.09 respectively and it was determined that

$$S_{\max} = 0.2 h_{\text{sea}}. \quad (5)$$

No universal value was found for h_{sea} so site-specific values were found by least squares fit to data sets for each site. x_{\max} is the x location at which the exponential function is a maximum.

While S describes the amplitude of bars as a function of depth, the cosine term, $\cos[\theta(h_0)-\psi(t)]$, models the actual sand bar form. The bar phase structure can be found as

$$\theta(x) = \int_{x_{\text{off}}}^x \frac{2\pi}{L(x)} dx \quad (6)$$

where $L(x)$ is the spatially-variable bar wavelength and the integral starts from the offshore limit of the domain and proceeds inward to every x , using the depth, h_0 , at each x location. Bar wavelengths are surprisingly well predicted by an empirical relationship

$$L(h_0) = a_L \exp(b_L h_0(x)) \quad (7)$$

where best fit values of a_L and b_L are found to be 100 and 0.27, respectively.

The temporal phase, $\psi(t)$ is determined from the fact that bar crests (minimum depths) will occur when the argument of the cosine equals zero. Thus, if we can independently identify a bar position, x_b , we can find

$$\psi(t) = \theta(x_b) \quad (8)$$

where θ was found using equation (6). The final sum of the background and barred profile (eq. 1) is referred to as the “barred profile” and can be directly compared to measured bathymetries.

As was discussed in HLEV14, of the twelve parameters needed for implementation, seven were evaluated as constants in RWHKvE03. Four of the remaining five are determined by: the climatological beach slope at the shoreline, the depth and bottom slope at some location seaward of the active bar zone (likely obtainable from nautical charts), and the cross-shore location of the sand bar crest determined from, for example, the breaker location from optical images of the nearshore. The final parameter, h_{sea} , is site-dependent and must be estimated. In the absence of other information, equation 5 can be used based on an estimate of the maximum expected height of sand bars at any site of interest.

2.2 2D Implementation

Natural beaches can only rarely be considered longshore-uniform. Shoreline locations vary on a range of scales from cusps to large-scale shoreline curvature and sand bar position are typical longshore-variable with a variety of morphologies [e.g. *Wright and Short*, 1983]. These longshore bathymetric variations change nearshore circulation in important ways [e.g. *Wilson et al.*, 2010 among many others], yielding rips currents and cell circulation that are important to mixing and morphological evolution.

One concept for extending HLEV14 to two dimensions is to simply take profiles that are orthogonal everywhere to a longshore-variable shoreline orientation and averaging the

1
2
3
4 offshore results with a spatial smoothing. However this method was discarded after it
5
6
7 was found to be unstable and overly sensitive to details of shoreline orientation (depth
8
9 estimates at any offshore location could be averages from a random mix of originating
10
11 shoreline transect locations).
12
13
14

15 Instead, the following method was found to work. Instead of computing a suite of
16
17 offshore transects for every shoreline position then averaging at every offshore
18
19 position, it was assumed that each estimation point seaward of the shoreline “sees”
20
21 the coast as roughly straight with an orientation that is the average over a longshore
22
23 span whose length depends on the offshore distance. For large offshore distances,
24
25 the coastal orientation should be thought of as the average over a large span
26
27 whereas close to the beach the orientation is more localized. Given this mean
28
29 coastal orientation, a normal transect can be determined between the estimation
30
31 point and the corresponding averaged shoreline. From the intersection of this
32
33 transect with a bar and offshore location a full barred bathymetry can be computed
34
35 using HLEV14 from which the depth at the estimation point can be found. This is
36
37 carried out one point at a time over a full 2D estimation grid (this may seem like a
38
39 lot of wasted computation but bathymetries presented below took only an average
40
41 of 120 s to compute on an average laptop).
42
43
44
45
46
47
48
49
50
51

52 The concept is illustrated in Figure 1 where we are trying to estimate the depth at a
53
54 particular offshore point, $[x_p, y_p]$, shown as a red asterisk in the figure. We assume
55
56 the shoreline has been digitized from a rectified aerial photograph as a series of
57
58 points, x_s, y_s and the foreshore beach slope has been estimated from local knowledge
59
60
61
62
63
64
65

1
2
3
4 as $\beta_s(y)$. We wish to define a mean shoreline that would be “seen” by the offshore
5
6 point as the best fit line (dashed near-vertical line in Figure 1) to the shoreline data
7
8 within $K \cdot dx$ of y_p , where dx is the distance between x_p and the mean of the subset of
9
10 shoreline x locations. For illustration we have used $K=1$ (other choices are
11
12 investigated later). Figure 1 shows the selected subset of shoreline data as a red
13
14 curved line (from $y_p - K \cdot dx$ to $y_p + K \cdot dx$) while the dashed red line shows the best
15
16 linear fit to these points. This problem must be solved iteratively (guessing an
17
18 offshore distance, then finding the shoreline subset, then improving the estimate of
19
20 dx , until convergence).
21
22
23
24
25
26

27
28 Having identified a linear shoreline that is appropriate to a particular offshore
29
30 location, the subsequent analysis is straightforward. A normal is found to the
31
32 shoreline (solid straight red line in Figure 1, having an orientation of $-1/m$, where m
33
34 is the slope of the shoreline fit line, $x = my + b$). The intersection of the straight
35
36 shoreline with this normal is found as x_0, y_0 , and the along-transect distance, d , is
37
38 found between this point and x_p, y_p . The along-transect distance, d_b , is found to the
39
40 sand bar and the distance, d_d , is found to the deep contour. The offshore depth and
41
42 slope at the deep location are found. From these values, a 1D barred profile can be
43
44 found as in HLEV14 and the depth at along-transect distance, d , is interpolated. This
45
46 process is carried out for every location in an analysis map grid that is seaward of
47
48 the shoreline. Note that the intersection of the cross-shore transect with the bar or
49
50 deep contours requires finding the two-line intersection for every line segment
51
52
53
54
55
56
57
58
59
60
61
62
63
64
65

1
2
3
4 along the bar (or deep) contour and choosing the one that lies within the line
5
6 segment (i.e. most will intersect outside of the domain of each point pair).
7
8
9

10 11 **3. Field Data Tests**

12 The above parametric barred beach form was compared against fourteen 2D beach

13 surveys carried out at the FRF, Duck, North Carolina, under widely varying
14

15 environmental conditions between September 2009 and May 2011 (dates listed in
16

17 Table 1). Survey data were collected along 26 cross-shore transects with an
18

19 alongshore spacing of 50 m and a typical cross-shore sample spacing of 3.5 m.
20

21 Transects extended from the dune base to 800 m offshore, with five transects
22

23 extending to 2000 m. An example of the survey coverage is shown in Figure 2.
24

25 Birkemeier and Mason [1984] found that the vertical accuracy of FRF surveys is
26

27 approximately 0.05 m. The local x coordinate extends in the cross-shore direction
28

29 while y is oriented alongshore in a right hand coordinate system with z positive up.
30

31 Survey data were interpolated onto a 5 by 10 m (cross and alongshore spacing) grid
32

33 using loess interpolation with 25 and 50 m cross-shore and longshore smoothing.
34
35
36
37
38
39
40
41
42
43
44

45 The necessary inputs for the parametric model were found as follows. For initial
46

47 testing, the shoreline and bar crest locations were found from measured
48

49 bathymetries (initiation from time exposure images is discussed later in the paper).
50

51 The shoreline was defined as the location for which depth equals mean sea level ($z =$
52

53 0). The bar crest location was determined as the first depth minimum seaward of
54

55 the shoreline, with manual supervision to correct transects with monotonic depth
56

57 increase. Longshore spacing was chosen to be 50 m, but is arbitrary (Figure 2).
58
59
60
61
62
63
64
65

Following the values chosen in HLEV14, the foreshore climatological beach slope, β_s , was taken as 0.10, the mean over all surveys (from HLEV14), while the value of h_{sea} was taken to be 4.5 m. The deep water variables were chosen from example survey data (but could easily have been taken from charts) as depth of 7.5 m at $x = 700$ and offshore bottom slope, β_0 , of 0.0088. Offshore depths were assumed alongshore uniform. K was taken to be 1.0.

Figure 3 shows an example comparison between a surveyed and a parametric bathymetry for October 21, 2009, a case of moderate longshore variability in shoreline and sand bar position. Anomalies in the surveyed bathymetry near $y = 500$ m, due to the known scour trench under the FRF pier, are poorly sampled in the survey and are not representative of natural beach processes. Performance statistics (below) therefore neglect the region between longshore distances 400 and 600, as is common practice.

The parametric bathymetry looks very similar to the survey, especially in shallow water. The overall structure of the shoreline and bar are well represented and longshore variations in the trough are reasonable. A low-amplitude offshore bar is present but is slightly deeper than in the survey. Figure 4 shows a difference plot of parametric minus survey depths (positive values correspond to over-estimates of depth in the parametric bathymetry) while Figure 5 shows transects of parametric and surveyed estimates at four longshore locations. Overall, the parametric form does a very good job of representing the 2D survey bathymetry. The most visually

1
2
3
4 apparent error (aside from the deep trench below the pier) is due to a slight
5
6
7 misplacement of the cross-shore bar position (between $x = 150$ and 200 m). To
8
9
10 seaward ($x \sim 350$ m) the parametric form over-predicts depth by roughly 1 m to the
11
12 south but is surprisingly accurate to the north ($y = 600, 800$ m).
13
14

15
16 Figure 6 shows a histogram of the prediction error. The slight bias toward over-
17
18 prediction of depth is apparent, but there are no particularly large anomalies. The
19
20 bias and rms error over the full domain are 0.30 and 0.47 m, respectively. The
21
22 bias and rms error over the full domain are 0.30 and 0.47 m, respectively. The
23
24 median value of the absolute error was 0.29 m while the 90% percentile of absolute
25
26 error was 0.77 m (i.e. 90% of errors were less than this value). The error statistics
27
28 were also partitioned by depth to determine if performance was better in shallow (h
29
30 < 3 m) or deeper ($h > 3$ m) regions. Both bias and rmse were essentially depth
31
32 independent for this case.
33
34
35
36
37
38

39 Statistics for each of the fourteen surveys are shown in Table I. The results are quite
40
41 consistent from survey to survey. On average, the bias is a 0.27 m over-prediction
42
43 with an rms error of 0.49 m. The average median and 90^{th} percentile absolute
44
45 errors are 0.28 and 0.86 m, respectively. The bias is slightly lower in shallow water
46
47 (< 3 m; 0.24 versus 0.28 m) while the rms error is essentially the same in both
48
49 regions (0.50 versus 0.48).
50
51
52
53
54
55

56 Figure 7 shows the most complex bar system in the data set (09/16/09) while
57
58

59 Figure 8 shows the corresponding comparison of parametric and surveyed
60
61
62
63
64
65

1
2
3
4 bathymetries. The 2D parametric bathymetry is a very good approximation of the
5
6 survey, with error statistics that are roughly the same as the global averages (Table
7
8 I).
9

10
11
12
13
14 Figure 9 shows one further case from 04/16/10, another case where the survey
15
16 bathymetry shows strong longshore variability. The parametric bathymetry
17
18 represents well the alongshore variability but cannot represent rip channels that
19
20 have been cut through the bar at $y = 190$ and 750 m.
21
22
23
24
25

26
27 The best value of K is unknown. A value smaller than the default value of 1.0 would
28
29 make the parametric bathymetry more sensitive to shoreline details while a large
30
31 value reduces this sensitivity. Performance statistics were computed for values of K
32
33 of 0.5 and 2.0 , so spanning a factor of four. The statistics of the fit were found to be
34
35 quite insensitive (Table II).
36
37
38
39
40

41
42 It should be realized that for a generally straight beach such as Duck, shoreline
43
44 curvature could be reasonably ignored - after all, the results of HLEV14 were all
45
46 based on 1DH cross-shore transects with no sensitivity to shoreline curvature.
47
48 However, there are negative consequences of adapting the 1DH approach for
49
50 longshore variable beaches. First, every detail of shoreline variability will be carried
51
52 throughout the profile, so the position of the crest of an offshore sand bar will vary
53
54 just as much as the shoreline, an unrealistic behavior (although subtle in terms of
55
56 error since offshore features are usually low sloping). Second, for cases with more
57
58
59
60
61
62
63
64
65

significant shoreline curvature like a pocket beach, the sensible variability of shore normal direction is required for realistic bathymetry and hydrodynamics.

For real applications, the surveyed bathymetry will be unknown (why would you then approximate it?). Thus, shoreline and sand bar input data must be found in other ways, most likely from remote sensing data. This was tested by using rectified time exposure images collected by the Duck Argus Station (for example, Figures 2 and 7) and manually digitizing the shoreline and sand bar locations by clicking on the image. This has previously been shown to provide a good approximation, although some cross-shore misplacement can occur depending on the wave conditions [e.g. *Lippmann and Holman, 1989; Plant and Holman, 1997; van Enckevort and Ruessink, 2001*]. This was done for each of the fourteen survey times. For several cases, waves were too small to break over the sand bar on the survey date so the closest time exposure with usable signals was chosen, sometimes up to three days different from the ground truth survey date (time exposure dates are listed in Table I). Parametric bathymetries were computed for each case and the statistics found (last line, Table II). Surprisingly, bulk statistical performance was no worse using these approximate inputs than using those derived from surveyed bathymetries.

4. Discussion

The 2D parametric algorithm does a very good job producing realistic bathymetries based only on simple inputs of shoreline and sand bar locations, a shoreline climatological slope and some offshore depth and slope at a location that is seaward

1
2
3
4 of the active sand bar region (anywhere seaward of 8 m depth is usually adequate).
5
6
7 These predictions are a great improvement over traditional power law or
8
9 exponential beach forms due to the inclusion of sand bars that will strongly
10
11 influence nearshore wave breaking and the resulting circulation. The parametric
12
13 form can well represent the longshore variability that is important for causing rips
14
15 currents and cell circulation although rip channels that are cut through a sand bar
16
17 cannot be modeled.
18
19
20
21
22

23
24 The algorithm can be used in two general ways. The first is for general or even
25
26 conceptual studies where the user simply needs a realistic bathymetry to study
27
28 processes. This is the traditional role of equilibrium beach profiles – for instance,
29
30 the $x^{2/3}$ profile is often used for this type of study since it represents the typical
31
32 concave average bathymetry of ocean beaches. However the lack of the sand bars
33
34 makes hydrodynamic predictions on these simpler profiles unrealistic. Since no
35
36 sand bar location is known, different bar placements can be explored at will. The
37
38 second application is to represent a specific beach for which measured bathymetry
39
40 is poor or completely lacking. This is often the case for Navy applications where
41
42 bathymetry is needed for operational planning but is unavailable. This algorithm
43
44 could provide a realistic substitute based only a few inputs that could reasonably be
45
46 estimated or guessed. Of course, the estimated bathymetries would not be as good
47
48 as measurements, but they are surprisingly good.
49
50
51
52
53
54
55
56
57
58
59
60
61
62
63
64
65

1
2
3
4 The largest numerical errors are often due to a cross-shore misplacement of the
5
6 sand bar position (for instance the slight misplacement of the bar location in Figure
7
8 3 and resulting alongshore anomaly between $x = 150$ and 200 m in Figure 4). The
9
10 associated increase in the error statistics due to a realistic bar form shifted slightly
11
12 in the cross-shore is misleading since both the bathymetric form and any resulting
13
14 hydrodynamics will still be realistic but slightly shifted in the cross-shore.
15
16
17
18
19
20

21
22 Digitization of shoreline and sand bar locations from optical imagery is necessarily
23
24 subjective. For a steep beach like Duck, the shoreline can usually be fairly
25
26 accurately found. However, at other times and locations a small low tide terrace can
27
28 be present and shorelines must be estimated to the landward of the terrace break
29
30 (e.g. around $y = 600$, Figure 7). Both the shoreline and sand bar location digitization
31
32 should be based on mean tide time exposure images since both signals will vary
33
34 with the tide. However, preference in this case was given instead to finding time
35
36 exposure images that best showed usable breaking patterns over the offshore sand
37
38 bar location (usually a low tide).
39
40
41
42
43
44
45

46
47 Most practical applications of this algorithm will be based on snapshots of wave
48
49 breaking rather than time exposure images. Figure 10 shows a rectified snapshot
50
51 from 10/21/09, the initial case discussed above. White dashed lines correspond to
52
53 the shoreline and sand bar locations digitized from the surveyed bathymetry in
54
55 Figure 3. In this case there is sufficient signal in the single snapshot to allow
56
57 reasonable estimates of shoreline and sand bar locations. In general the use of
58
59
60
61
62
63
64
65

1
2
3
4 snapshots rather than time exposures should degrade the final product somewhat.
5
6
7 However a user should be able to judge the merit of their choices. In all cases, the
8
9 most likely resulting error will be a cross-shore misplacement of sand bars and the
10
11 resulting bathymetries and hydrodynamics will still be more realistic than for
12
13 unbarred bathymetries.
14
15
16
17
18
19

20 The current version of the analysis assumes that the longshore direction
21
22 corresponds roughly to the y-axis, i.e. the shoreline, bar and deep input data can be
23
24 reasonably expressed as a function of y. Under more complex situations, other
25
26 choices may need to be made, for example to frame the problem as a function of a
27
28 series of longshore line segments. Similarly, the alongshore spacing of input data is
29
30 arbitrary. It must be dense enough to represent important shoreline variability and,
31
32 while densely spaced inputs are fine, they may needlessly increase computation
33
34 time. The computation time for these cases averaged 120 s using a low level
35
36 desktop computer.
37
38
39
40
41
42
43
44

45 The algorithm depends on and may be sensitive to a number of parameters. The
46
47 most sensitive is h_{sea} , the seaward limit of significant sand bar activity. HLEV14
48
49 investigated this dependence and found that increasing h_{sea} lead to a larger
50
51 amplitude sand bars that continued further seaward. This would lead to errors
52
53 offshore but would have little impact closer to the beach where the surf zone is most
54
55 active and interesting. In the absence of any information on the best choice for h_{sea} ,
56
57
58
59
60
61
62
63
64
65

1
2
3
4 it is possible to estimate the maximum expected amplitude of sand bars and use
5
6 equation (5) to find h_{sea} .
7
8
9

10
11 Errors in the shoreline location have obvious consequences of spatially offsetting
12 the resulting bathymetry. Similarly, errors in the depth at some offshore location
13
14 simply deepen or shallow the profile slightly with small resulting effects in bar
15
16 positioning away from the input sand bar location. However, the input bar position
17
18 will usually be one that is detected in shallow water, the location where conditions
19
20 are usually of the greatest interest, so this is a fairly innocuous error. The remaining
21
22 unknown sensitivities are due to errors in the shoreline and offshore slopes.
23
24
25
26
27
28
29

30
31 The role of the shoreline beach slope, β_s , is shown in Figure 11. The primary effect
32
33 of changing β_s is to change the depth in the trough region, close to the beach. The
34
35 location of the bar is unchanged (since it is an input), although the bar crest depth is
36
37 slightly affected.
38
39
40
41
42
43

44 The role of the deep-water slope, shown in Figure 12, is larger. The active bar zone
45
46 and the amplitudes of sand bars are dependent on the depth of the background
47
48 profile, h_0 , and are limited to a depth span from 0 to h_{sea} . Choosing a too shallow
49
50 offshore slope will make the cross-shore width of this region very narrow so that
51
52 bar perturbations will appear to be small (see $\beta = 0.006$ case in Figure 12). In this
53
54 sense, the choice of this slope has an indirect impact on the bar amplitudes. It is also
55
56 quite possible to choose an offshore slope that is too steep, so would intersect the
57
58
59
60
61
62
63
64
65

1
2
3
4 beach above sea level (i.e. the beach would need to be convex up to meet the
5
6 shoreline, a possible but unlikely scenario). In this case the algorithm defaults to a
7
8 background profile that is a plane beach between the deep point and the shoreline.
9
10 Realistic bars are still predicted.
11
12
13
14

15
16 The deep-water input can be located anywhere seaward of the active bar zone, even
17
18 kilometers away. It simply acts as a boundary condition for solving for the
19
20 background profile, h_0 . Choosing a distant location does not increase computation
21
22 time, although the greater the offshore distance, the less likely it is that shore
23
24 normal transects will intersect a spatially-limited deep water contour (this problem
25
26 can be resolved by inputting a very long offshore contour). Various options exist for
27
28 finding deep-water depths and slopes including digital nautical charts, alternate
29
30 remote sensing methods such as multi-spectral methods, or even rough estimates
31
32 from experienced geologists.
33
34
35
36
37
38
39
40

41 **5. Conclusions**

42 This paper describes and tests a method for approximating realistic 2DH nearshore
43
44 bathymetry in the absence of bathymetric measurements. It is an improvement over
45
46 simple monotonic equilibrium bathymetries due to the addition of realistic sand bars and
47
48 the associated great improvements in hydrodynamic predictions. It extends the 1DH
49
50 model of Holman et al [2014] in allowing for alongshore variability. Model inputs
51
52 include the position and climatological beach slope of the shoreline, the location of a
53
54 sand bar crest and the location and bathymetric slope at any offshore location that is
55
56 seaward of the zone of active sand bars.
57
58
59
60
61
62
63
64
65

The model was tested against 14 area surveys collected at Duck, NC, over a two-year period, each spanning 500 m in the cross-shore and 1000 m in the longshore. Input data for initial tests were extracted from survey data and a single historical deep-water survey with a later tests based on inputs extracted from remote sensing data. The mean bias over the entire region and data set was 0.27 m with an rms error of 0.49 m. Roughly 90% of the estimates were within 0.86 of the ground truth. The largest source of error was occasional cross-shore misplacements of otherwise realistic looking sand bars.

Hydrodynamic predictions using these bathymetries would be a substantial improvement over those from monotonic or even barred 1DH equilibrium proxy bathymetries.

6. Acknowledgements

The work was supported by the Office of Naval Research through base funding of the Naval Research Laboratory.

7 References

- Birkemeier, W. A., and C. Mason (1984), The CRAB: A unique nearshore surveying vehicle, *Journal of Survey Engineering*, 110, 1-7.
- Bodge, K. R. (1992), Representing equilibrium beach profiles with an exponential expression, *Journal of Coastal Research*, 8(1), 47-55.
- Bruun, P. (1954), Coast erosion and the development of beach profiles: Technical memorandum Rep.
- Dean, R. G. (1991), Equilibrium beach profiles: characteristics and applications, *Journal of Coastal Research*, 7, 53-84.
- Holman, R. A., D. M. Lalejini, K. Edwards, and J. Veeramony (2014), A parametric model for barred equilibrium beach profiles, *Coastal Engineering*, 90, 85-94.
- Inman, D. L., H. S. Elwany, and S. A. Jenkins (1993), Shorerise and bar-berm profiles on ocean beaches, *Journal of Geophysical Research*, 98(C10), 18181-18199, doi:10.1029/93JC00996.
- Komar, P. D., and W. G. McDougal (1994), The analysis of beach profiles and nearshore processes using the exponential beach profile form, *Journal of Coastal Research*, 10(59-69).
- Larson, M., and N. C. Kraus (1989), SBEACH: Numerical model to simulate storm-induced beach change Rep.
- Lippmann, T. C., and R. A. Holman (1989), Quantification of sand bar morphology: A video technique based on wave dissipation, *Journal of Geophysical Research*, 94(C1), 995-1011.

Ozkan-Haller, H. T., and S. Brundidge (2007), Equilibrium beach profile concept for Delaware Beaches, *Journal of Waterway, Port, Coastal and Ocean Engineering*, 133(2), 147-160, doi:10.1061/(ASCE)0733-950X.

Plant, N. G., and R. A. Holman (1997), Intertidal beach profile estimation using video images, *Marine Geology*, 140, 1-24.

Ruessink, B. G., K. M. Wijnberg, R. A. Holman, Y. Kuriyama, and I. M. J. van Enckevort (2003), Inter-site comparisons of interannual nearshore bar behavior, *Journal of Geophysical Research*, 108, doi:10.1029/2002JC001505.

van Enckevort, I. M. J., and B. G. Ruessink (2001), Effect of hydrodynamics and bathymetry of video estimates of nearshore sand bar position, *Journal of Geophysical Research*, 106(C8), 16,969 - 916,979.

Wilson, G. W., H. T. Özkan-Haller, and R. A. Holman (2010), Data assimilation and bathymetric inversion in a two-dimensional horizontal surf zone model, *Journal of Geophysical Research*, 115(C12), doi:10.1029/2010JC006286.

Wright, L. D., and A. D. Short (1983), Morphodynamics of beaches and surf zones in Australia, in *CRC Handbook of Coastal Processes and Erosion*, edited by P. D. Komar, pp. 35-64, CRC Press, Boca Raton.

Table Captions

Table I. Dates and error statistics of the fourteen tested bathymetries computed from $\Delta h = h_{\text{param}} - h_{\text{survey}}$ (so positive Δh corresponds to parametric estimates being too deep). Bias and rms statistics are listed both for the entire region (shore to $x = 700$ m) and split into shallow (true depths < 3 m) and deep (true depths > 3 m). Median and 90% percentile of $\text{abs}(\Delta h)$ are also shown.

Table II. Average performance statistics for different values of K (first three rows). The final row shows the performance statistics when the input shoreline and bar locations were manually picked from rectified time exposure images instead of the surveyed bathymetry.

Table 1

Bathy Date	Timex Date	Bias (m)			rmse (m)			Median (m)	90% (m)
		All	<3m	>3m	All	<3m	>3m		
09/16/09	09/16/09	0.30	0.19	0.34	0.47	0.39	0.49	0.30	0.77
10/21/09	10/21/09	0.30	0.30	0.30	0.47	0.48	0.47	0.29	0.77
12/10/09	12/13/09	0.28	0.33	0.26	0.49	0.64	0.43	0.30	0.85
01/14/10	01/14/10	0.21	0.11	0.25	0.41	0.40	0.42	0.25	0.75
02/22/10	02/25/10	0.21	0.08	0.25	0.51	0.40	0.53	0.30	0.92
04/05/10	04/04/10	0.26	0.08	0.32	0.50	0.37	0.53	0.28	0.87
04/16/10	04/15/10	0.28	0.09	0.34	0.52	0.40	0.54	0.29	0.87
06/04/10	06/07/10	0.25	0.07	0.31	0.48	0.39	0.51	0.31	0.87
09/06/10	09/09/10	0.33	0.34	0.33	0.51	0.51	0.51	0.34	0.87
10/19/10	10/22/10	0.34	0.36	0.33	0.54	0.54	0.53	0.29	0.95
11/22/10	11/24/10	0.29	0.21	0.33	0.54	0.56	0.54	0.30	0.97
02/07/11	02/05/11	0.27	0.31	0.26	0.52	0.56	0.50	0.22	0.97
03/18/11	03/18/11	0.25	0.47	0.16	0.49	0.69	0.38	0.23	0.87
05/02/11	05/02/11	0.22	0.35	0.17	0.44	0.59	0.36	0.21	0.77
MEAN		0.27	0.24	0.28	0.49	0.50	0.48	0.28	0.86

Table 2

K	Bias (m)			rmse (m)			Median (m)	90% (m)
	All	<3m	>3m	All	<3m	>3m		
0.5	0.27	0.23	0.28	0.49	0.49	0.48	0.28	0.86
1.0	0.27	0.24	0.28	0.49	0.50	0.48	0.28	0.86
2.0	0.27	0.24	0.28	0.49	0.50	0.48	0.28	0.86
Timex, K=1	0.25	0.10	0.29	0.49	0.48	0.49	0.29	0.86

Figure Captions

Figure 1. Schematic of example test case. The shoreline is shown in black (dotted line shows original points while the solid line shows the spline-interpolated shoreline). The blue line indicates the digitized sand bar location and the green line shows an assumed deep contour (chosen to be 12 m deep for this synthetic case). The red asterisk marks the particular analysis point, x_p, y_p . The red dashed line is the best-fit shoreline within the alongshore region of interest while the solid red line is the cross-shore transect (which defines a line that extends offshore to the deep contour).

Figure 2. Example rectified time exposure image for October 21, 2009. Blue points represent the tracks from the ground truth survey. The vertical feature at $y = 515$ m is the research pier. Shoreline locations extracted from survey data are shown by the white asterisks along the beach's edge while the estimated bar crest locations are the white asterisks overlying the white band of preferred breaking around $x = 200$ m.

Figure 3. Comparison of surveyed (right) and parametric (left) bathymetries. White lines show the shoreline and sand bar locations extracted from the survey data. The CRAB survey anomaly around $y = 500$ m is the poorly sampled trench below the pier and is ignored in statistical comparisons.

Figure 4. Difference plot of parametric minus surveyed depths for October 21, 2009. The narrow band of error between $x = 150$ and 200 corresponds to a slight misplacement of the inner bar crest location. The blue-ish region around $x = 350$ is a slight over-estimated of depth in the offshore bar region. The region between $y = 400$ and 600 m should be ignored.

Figure 5. Example profiles from Figure 3 at $y = 200, 400, 600$ and 800 m. Blue (red) lines correspond to parametric (survey) estimates.

Figure 6. Probability distribution of depth errors (predicted – survey) for the 10/21/09 survey. Positive values correspond to over-prediction of depth.

Figure 7. Rectified time exposure for 09/16/09, one of the most complex bar configurations in the study.

Figure 8. Parametric (left) and surveyed (right) bathymetries for 09/16/09. Despite the obvious three-dimensionality of the bar system and shoreline (Figure 7), the predicted bathymetry is quite good, with error statistics there are typical of all cases (Table I).

Figure 9. Predicted (left) and surveyed (right) bathymetries from 04/16/10.

Figure 10. Merged rectified snapshot that corresponds to the same time as the time exposure in Figure 3. White dashed lines again correspond to the shoreline and bar location digitized from the surveyed bathymetry. Wave breaking over the sand bar is more sporadic in the snapshot but would still yield quantifiable shore and bar locations.

Figure 11. Example profiles showing the sensitivity of predicted bathymetries on choices of shoreline beach slope, β_s .

Figure 12, the sensitivity of bathymetry to the chosen deep-water beach slope. For comparison, the value used for the Duck tests was 0.0088.

Figure 1

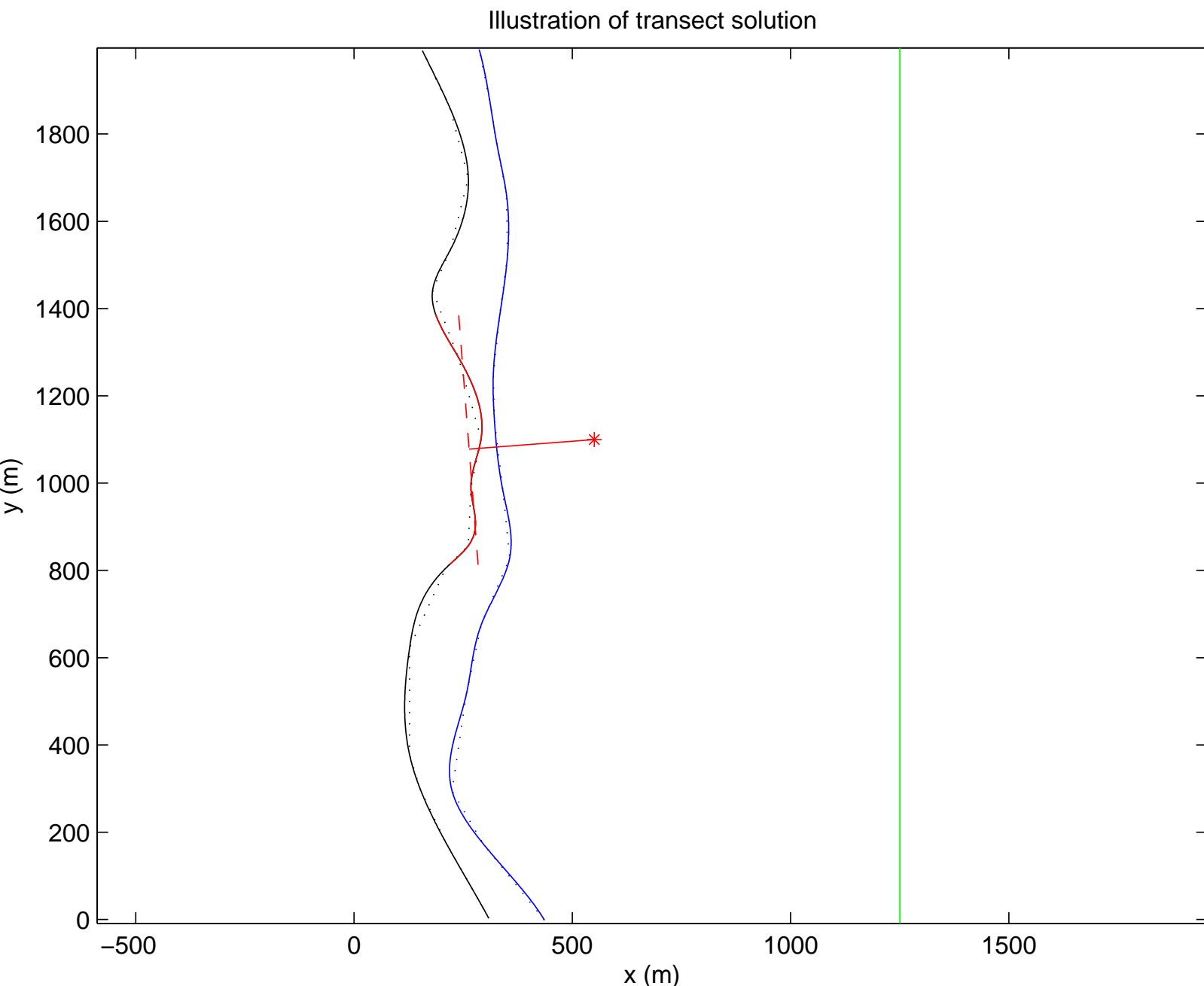


Figure 2

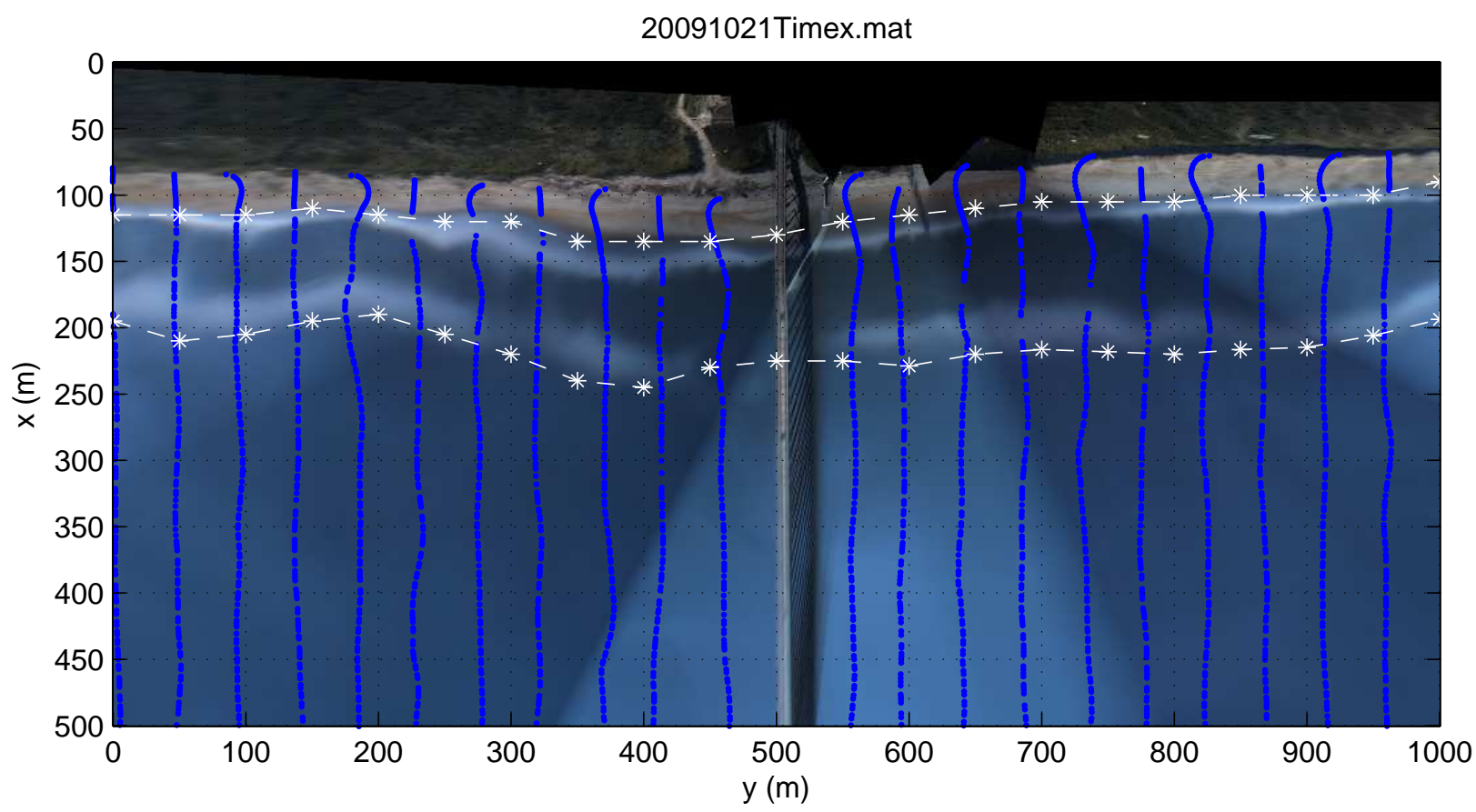


Figure 3

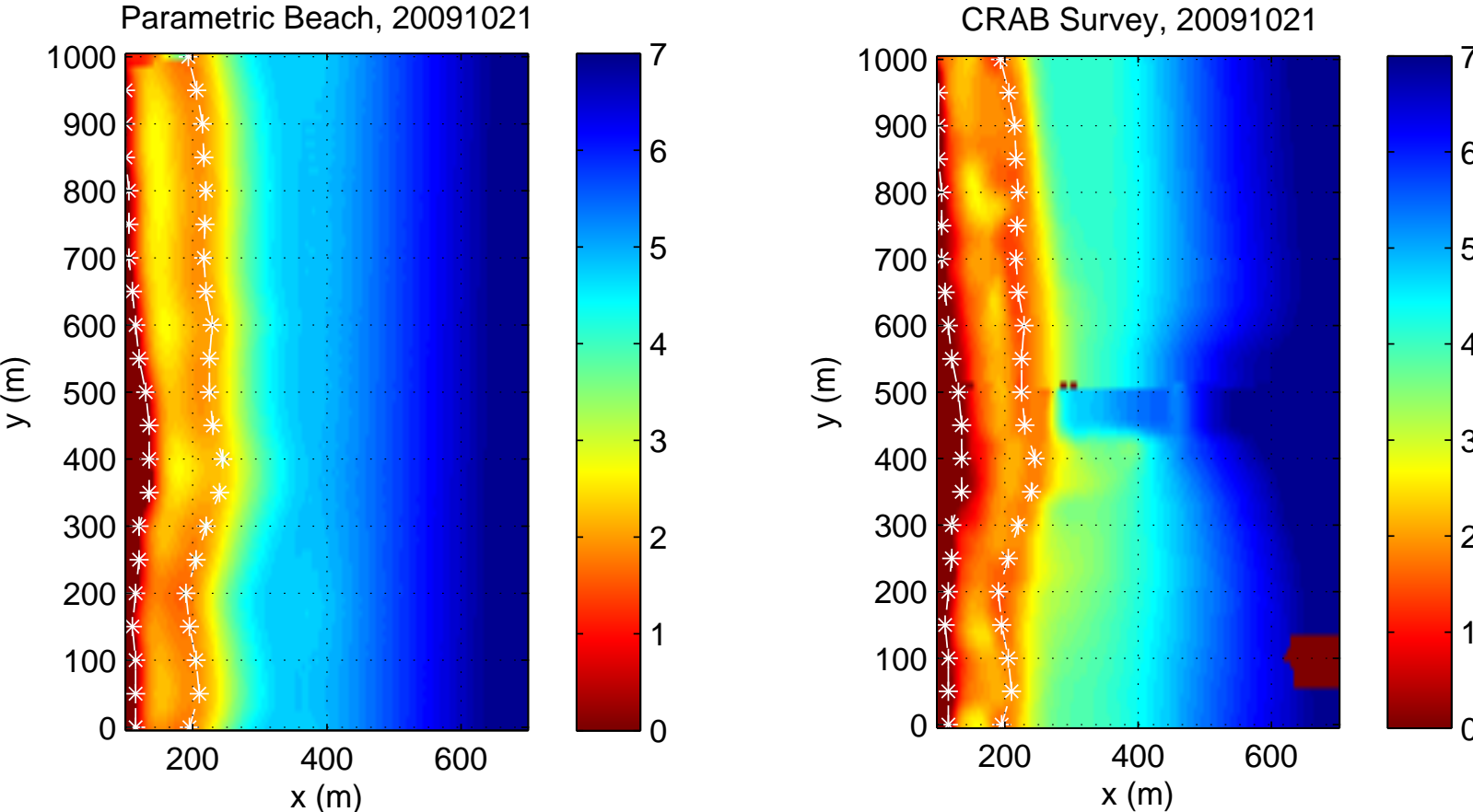


Figure 4

Parametric – CRAB Survey, 20091021

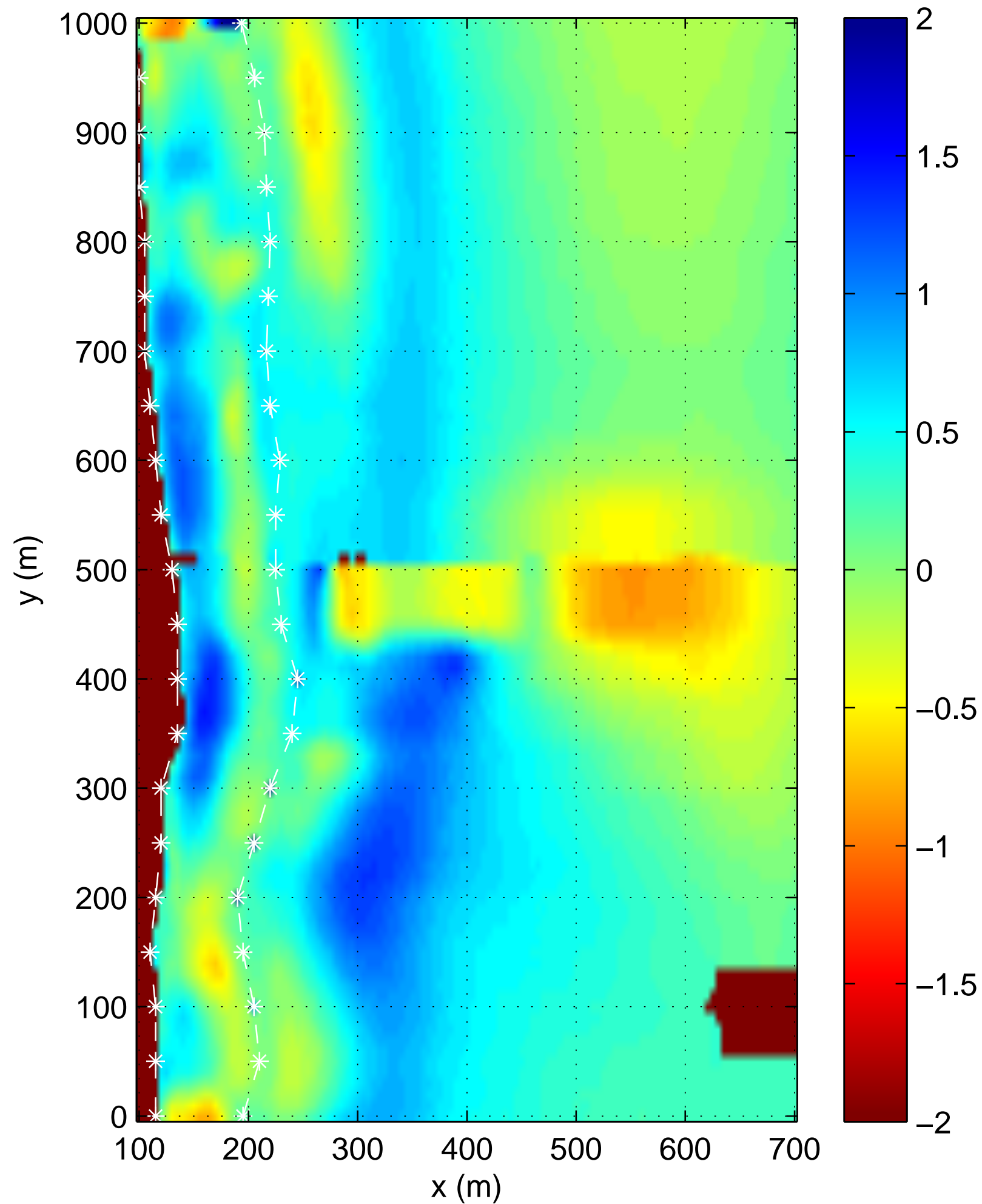


Figure 5

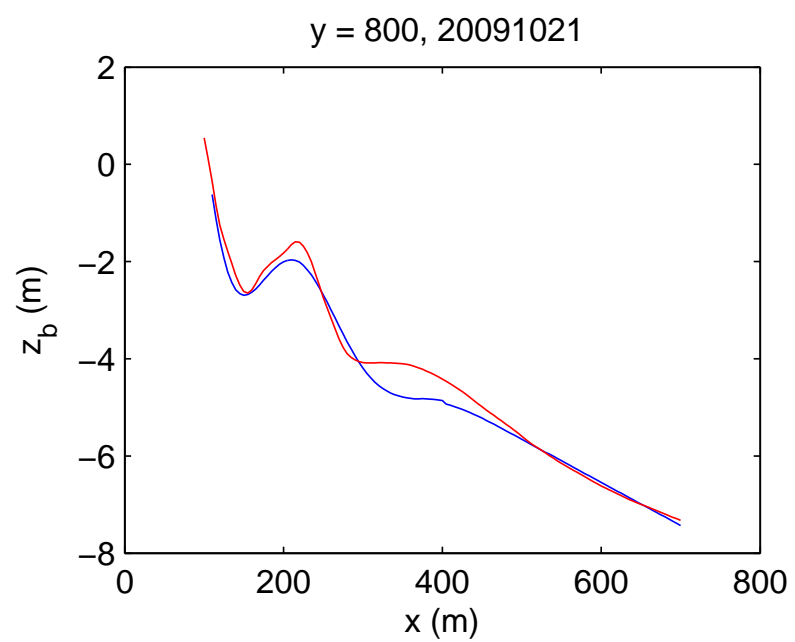
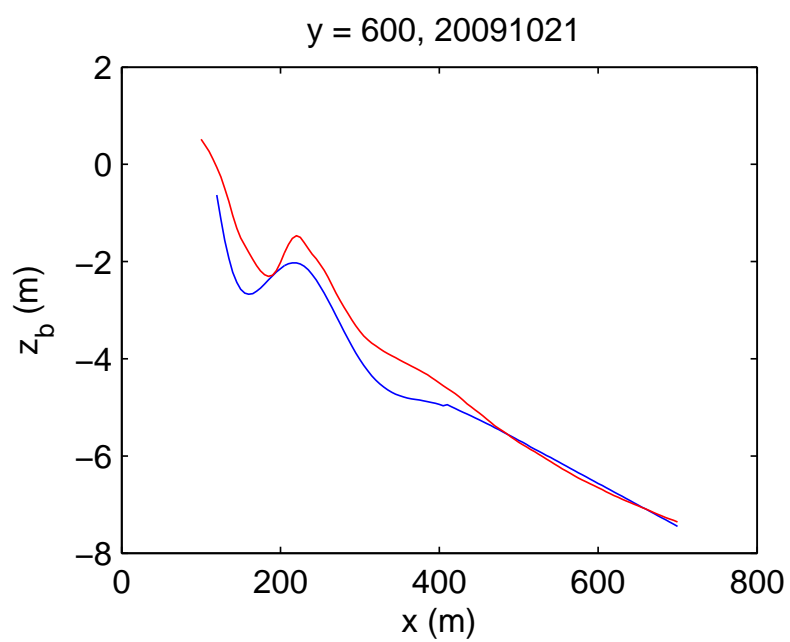
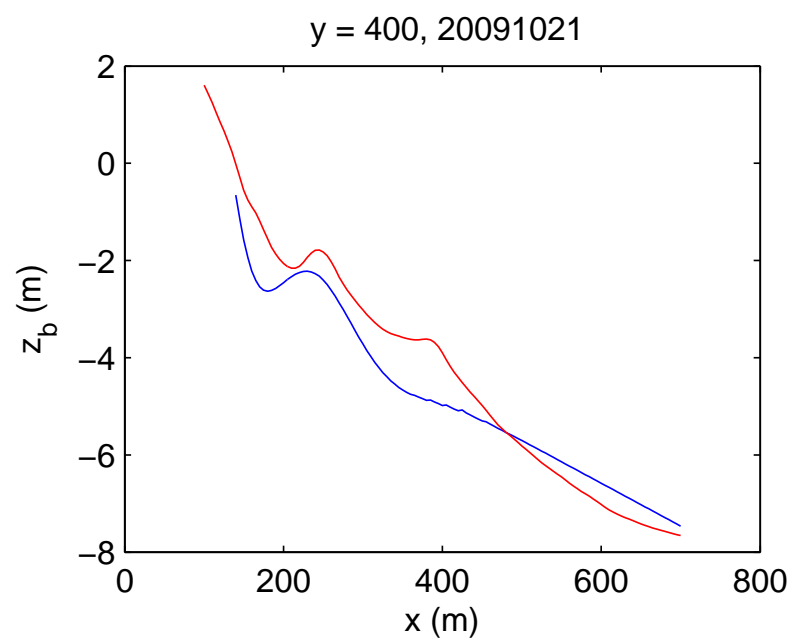
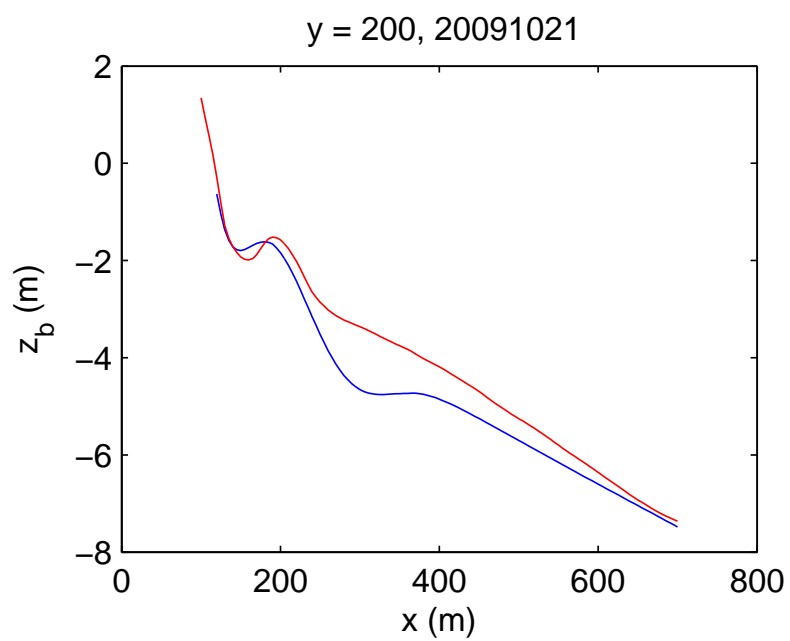


Figure 6

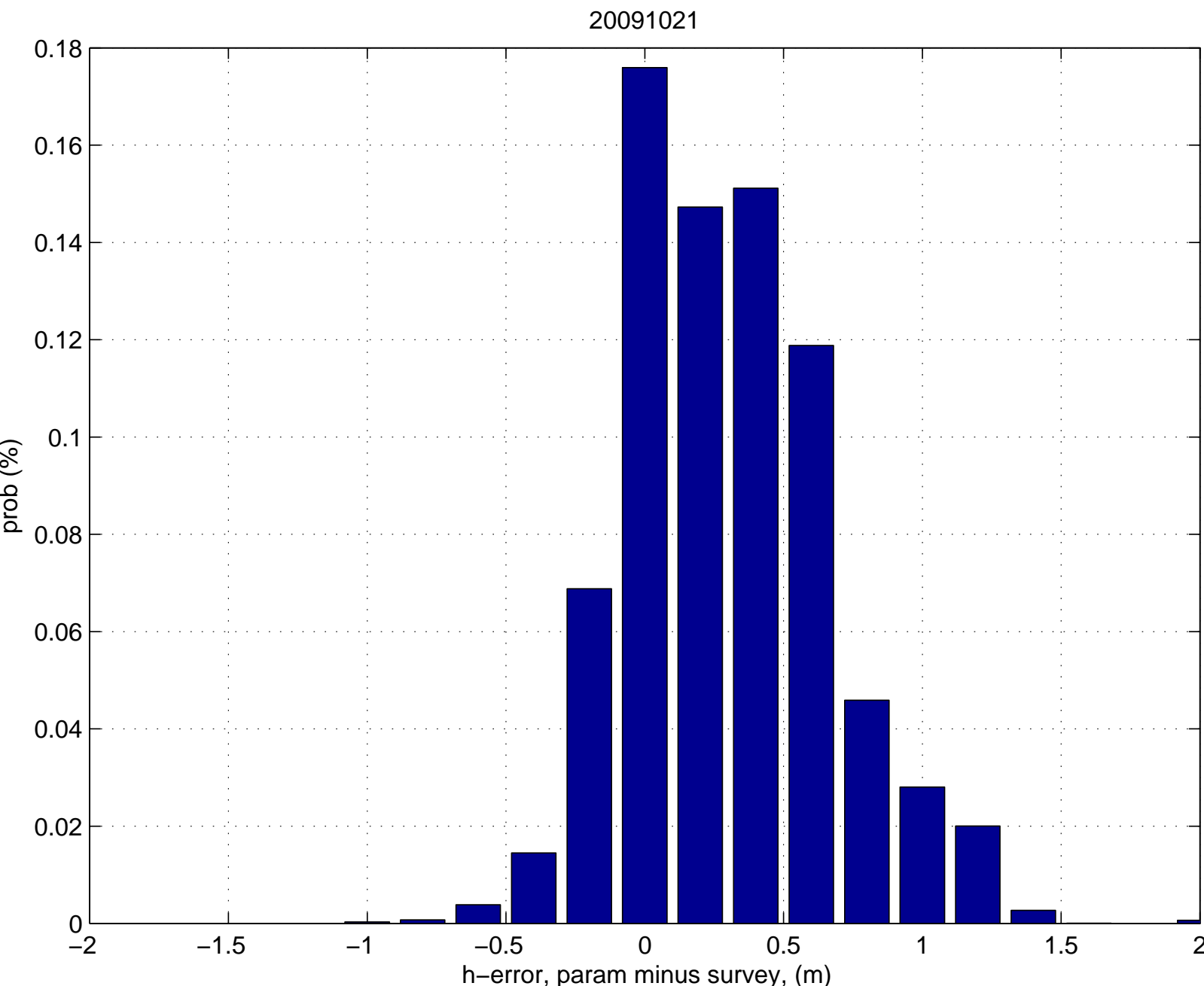


Figure 7

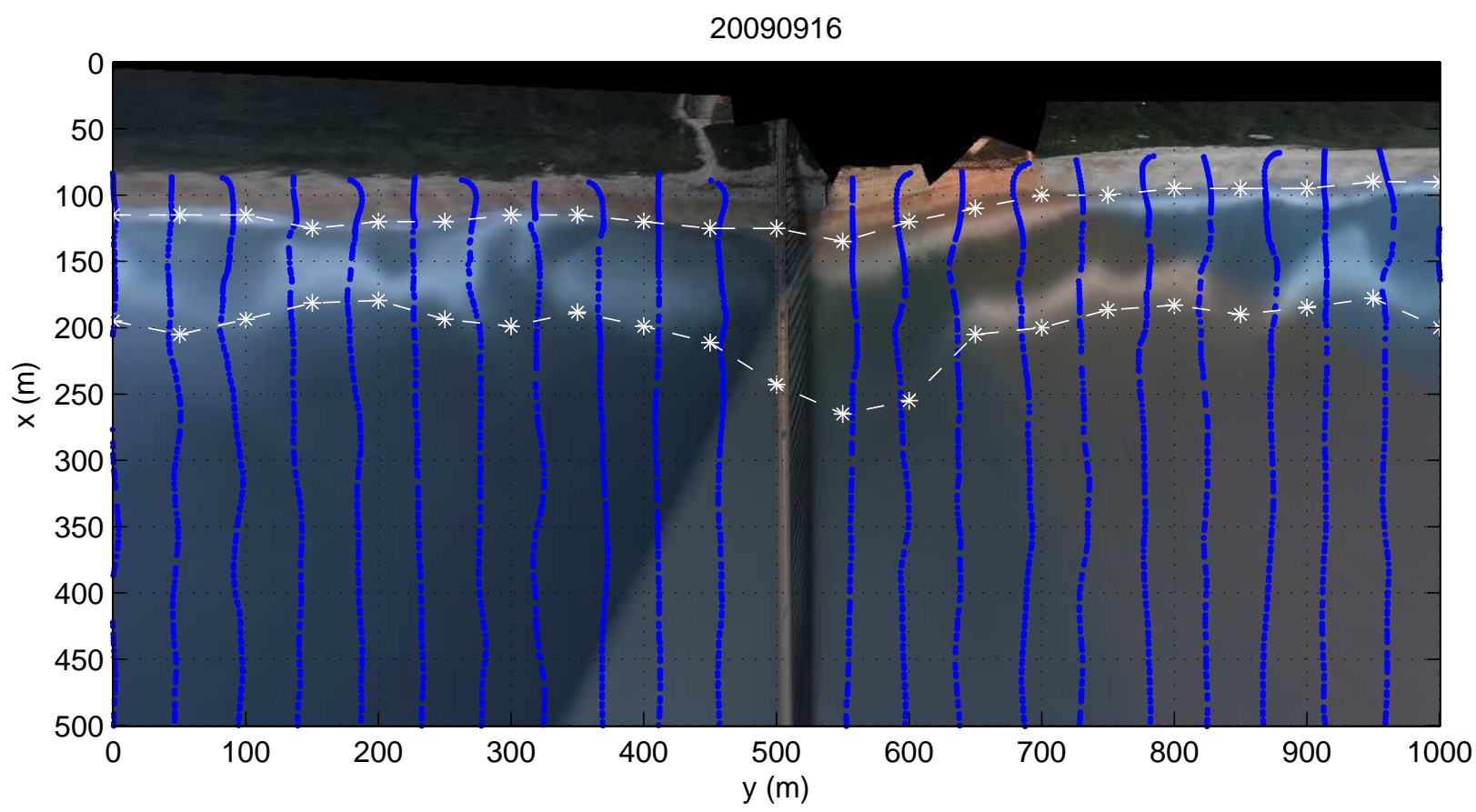


Figure 8

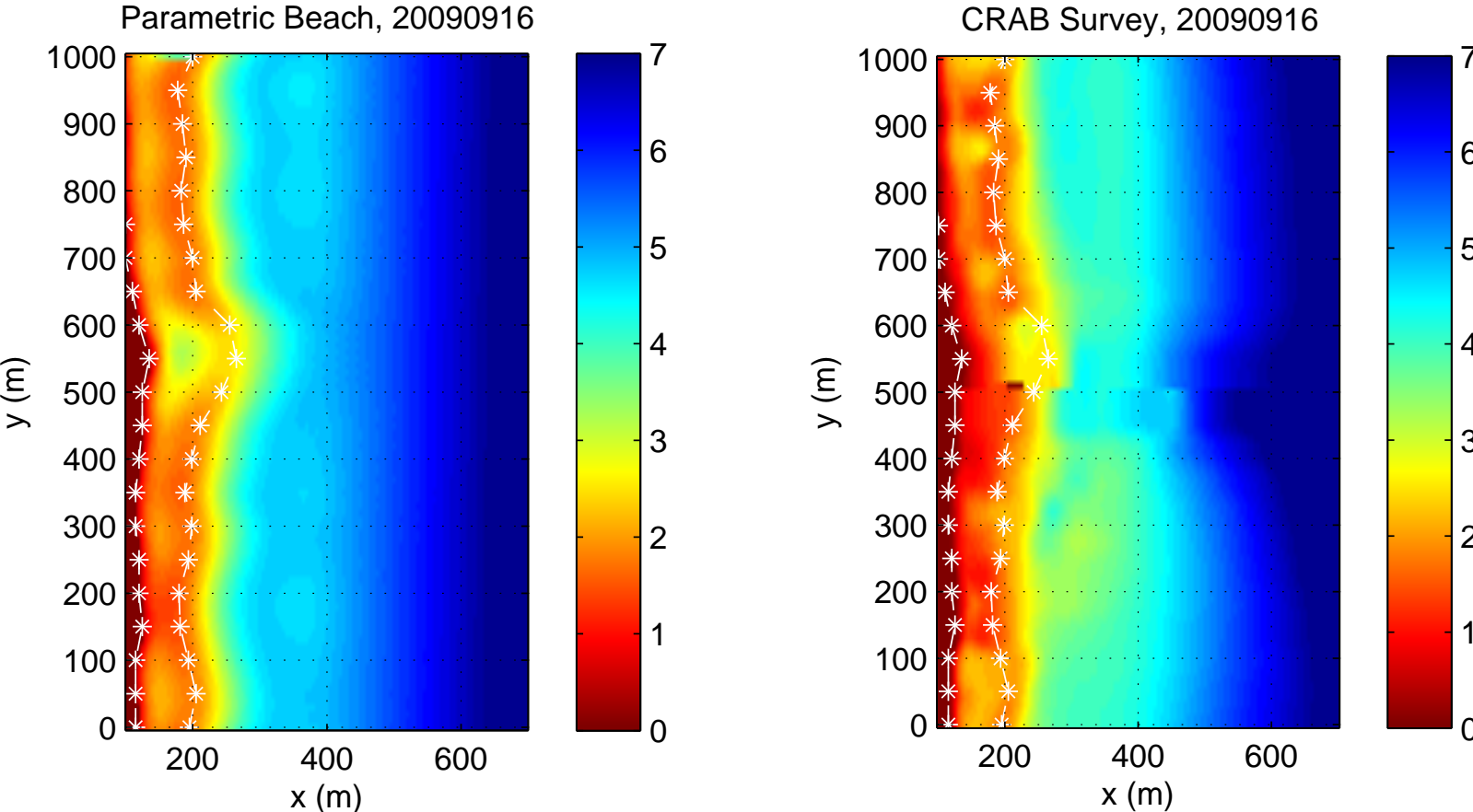


Figure 9

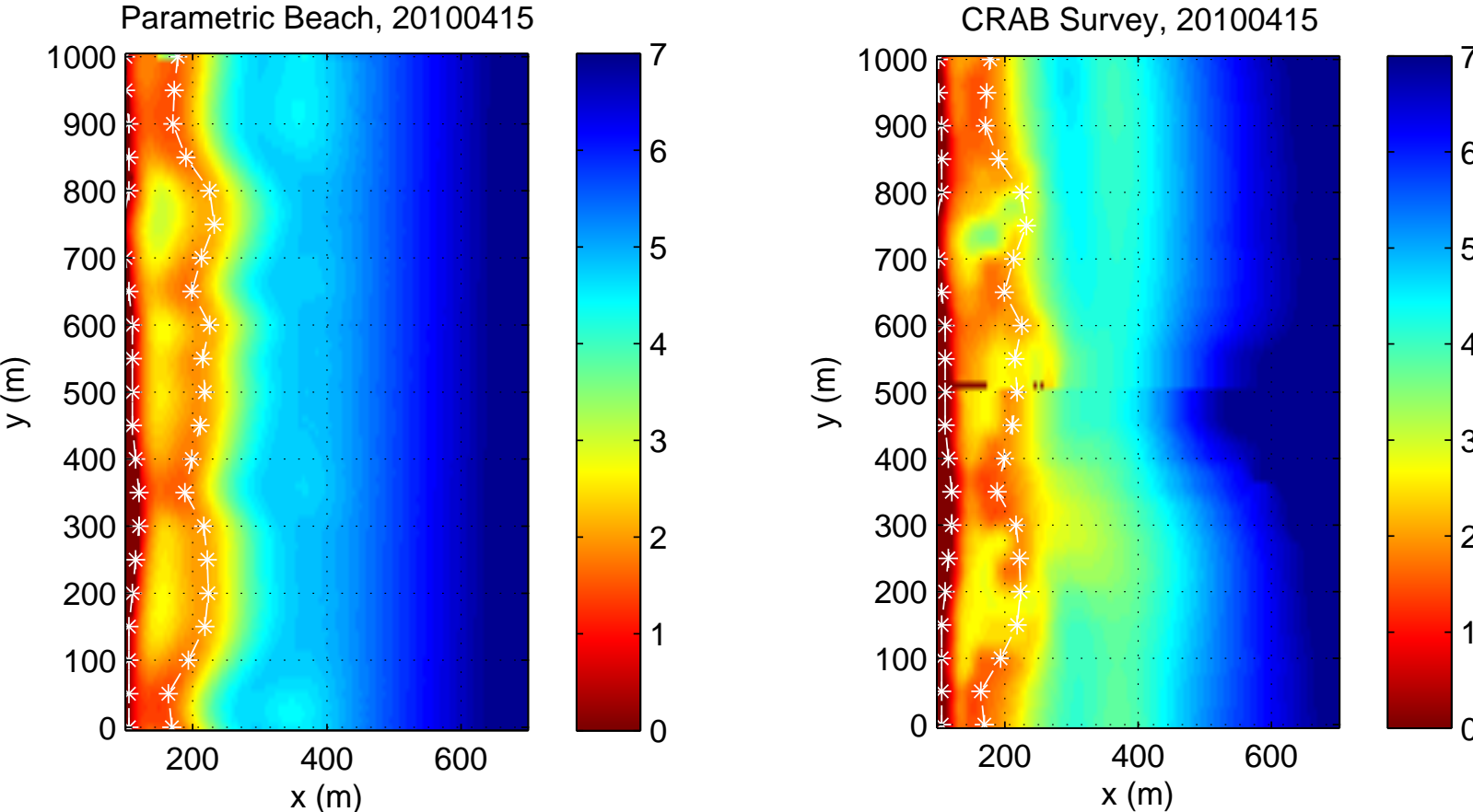


Figure 10

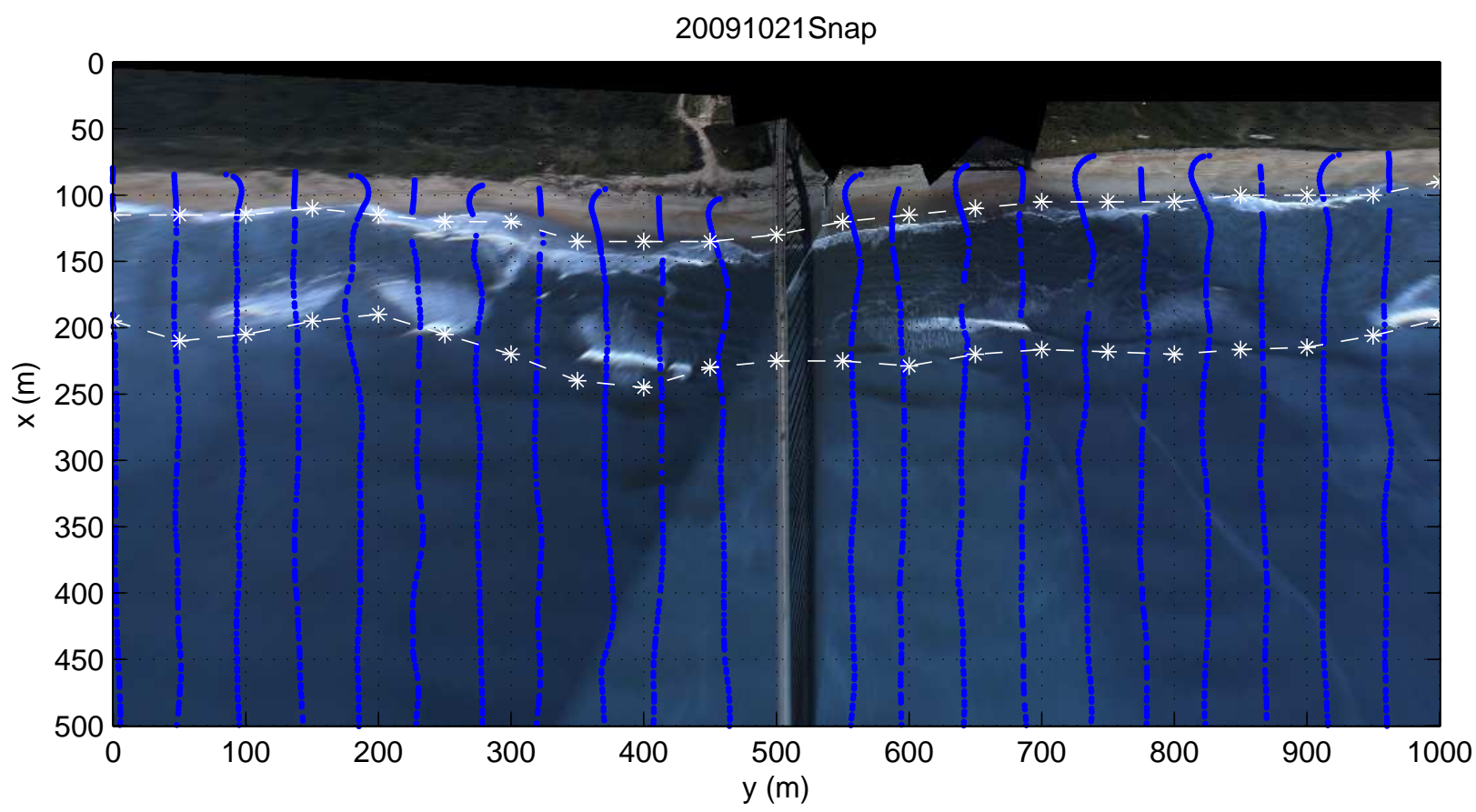


Figure 11

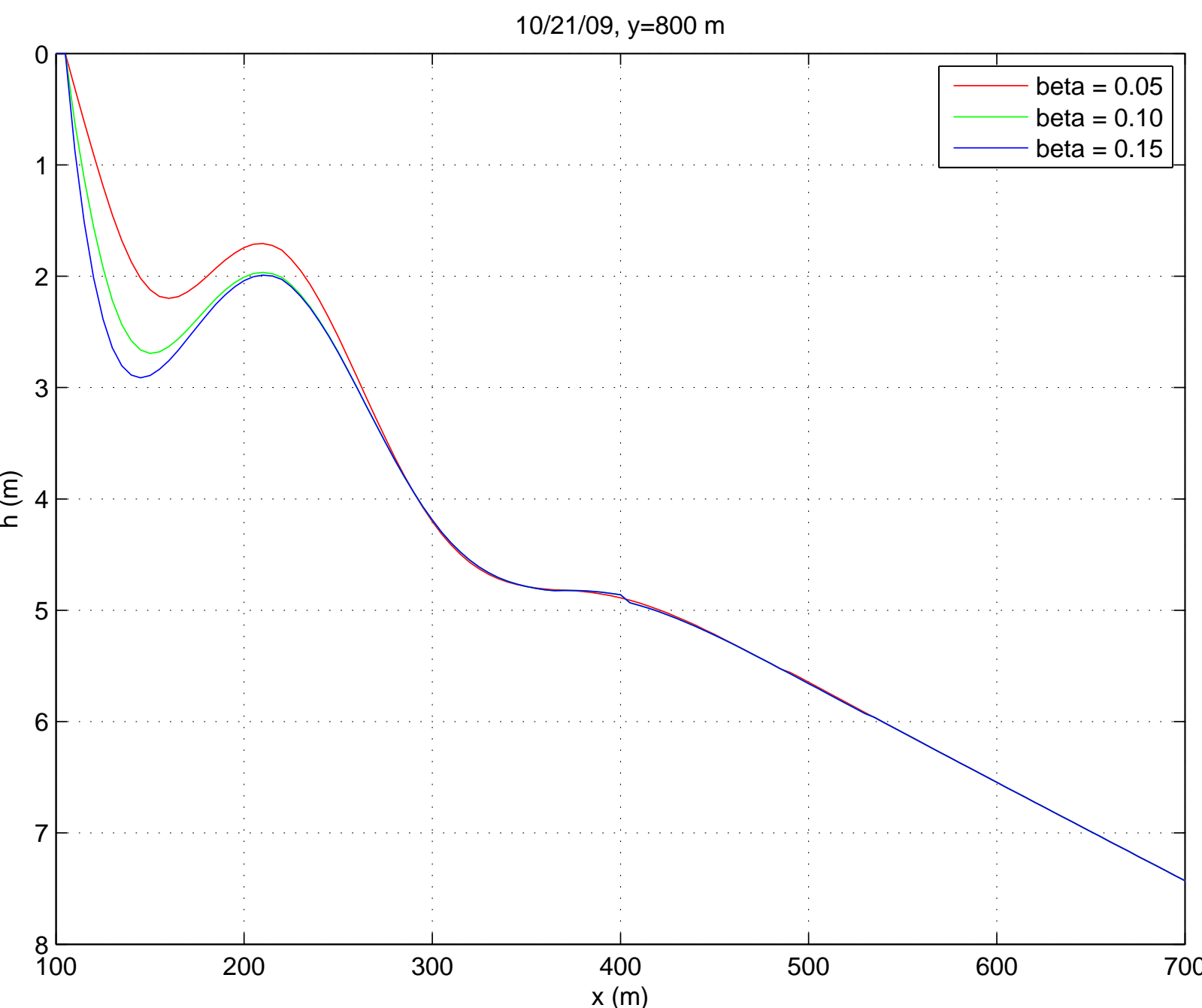


Figure 12

